ANTIOXIDANTS & REDOX SIGNALING
Volume 22, Number 7, 2015

DOI: 10.1089/ars.2014.5996

Discoveries

ORIGINAL RESEARCH COMMUNICATION

Vicious Inducible Nitric Oxide Synthase-Mitochondrial Reactive Oxygen Species Cycle Accelerates Inflammatory Response and Causes Liver Injury in Rats

Adelheid Weidinger,[1] Andrea Müllebner,[2] Jamile Paier-Pourani,[1] Asmita Banerjee,[1] Ingrid Miller,[2] Lothar Lauterböck,[2,*] J. Catharina Duvigneau,[2] Vladimir P. Skulachev,[3] Heinz Redl,[1] and Andrey V. Kozlov[1]

Abstract

Aims: Increasing evidences suggest that, apart from activation of guanylyl cyclase, intracellular nitric oxide (NO) signaling is associated with an interaction between NO and reactive oxygen species (ROS) to modulate physiological or pathophysiological processes. The aim of this study was to understand the contribution of mitochondrial ROS (mtROS) to NO-mediated signaling in hepatocytes on inflammation. ***Results:*** In rats treated with lipopolysaccharide (LPS), mitochondria-targeted antioxidants (mtAOX) (mitoTEMPO and SkQ1) reduced inducible nitric oxide synthase (*iNOS*) gene expression in liver, NO levels in blood and plasma, and markers of organ damage (lactate dehydrogenase, aspartate aminotransferase, and alanine aminotransferase). In cultured hepatocytes, treated with inflammatory mediators, generated *ex vivo* by incubation of white blood cells with LPS, we observed an increase in NO and mtROS levels. L-NG-monomethyl arginine citrate, a NOS inhibitor, decreased both NO and mtROS levels. mtAOX reduced mtROS, cytoplasmic ROS levels, and expression of *iNOS* and interleukin *(IL)-6*. These data suggest that NO, generated by iNOS, elevates mtROS, which, in turn, diffuse into the cytoplasm and upregulate *iNOS* and *IL-6*. ***Innovation:*** Here, for the first time, we show that intracellular signaling pathways mediated by NO and ROS are linked to each other *via* mtROS and form an iNOS-mtROS feed-forward loop which aggravates liver failure on acute inflammation. ***Conclusion:*** Our results provide a mechanistic explanation of how NO and mtROS cooperate to conduct inflammatory intracellular signals. We anticipate our results to be the missing mechanistic link between acute systemic inflammation and liver failure. *Antioxid. Redox Signal.* 22, 572–586.

Introduction

In the past, an interaction of nitric oxide (NO) with guanylyl cyclase was considered a principal regulatory function of NO (34), while an interaction of NO with superoxide radical ($O_2^{\bullet -}$) yielding peroxynitrite ($ONOO^-$) was considered a deleterious effect of excessive NO production (54). Recently, however, increasing evidence suggests that, apart from the activation of guanylyl cyclase, intracellular NO signaling is associated with the interaction between NO and reactive oxygen species (ROS) derived from $O_2^{\bullet -}$. In the majority of reports, the origin of ROS contributing to intracellular signaling is not identified, but several reports suggest mitochondria (4, 14, 16), NADPH oxidase (NOX) (39, 53), or xanthine oxidoreductase (XOR) (33) as possible sources. The primary reactive species formed in living cells are either $O_2^{\bullet -}$ or NO. $O_2^{\bullet -}$ can give rise to hydrogen peroxide (H_2O_2) and to hydroxyl radical. Interacting with NO, $O_2^{\bullet -}$ gives rise to $ONOO^-$. These four species predominantly operate in living systems and are termed ROS. H_2O_2 formed in mitochondria is a neutral molecule that can easily diffuse into the cytoplasm. $O_2^{\bullet -}$ has also recently been shown to leave

[1]Ludwig Boltzmann Institute for Experimental and Clinical Traumatology, Vienna, Austria.
[2]Institute for Medical Biochemistry, University of Veterinary Medicine, Vienna, Austria.
[3]A.N. Belozersky Institute of Physico-Chemical Biology, M.V. Lomonosov Moscow State University, Moscow, Russia.
*Current affiliation: Institute of Multiphase Processes, Leibniz University Hannover, Hannover, Germany.

Innovation

Overwhelming systemic inflammation often leads to multiple organ failure and death in critical illness, but the mechanistic progression of this phenomenon is still unknown, although the key role of mitochondrial dysfunction, excessive generation of reactive oxygen and nitrogen species was suggested. The major finding of this study is that we, for the first time, show that different segments of the inducible nitric oxide synthase-mitochondrial reactive oxygen species cycle, described separately in different experimental models, are actually not separated locally or functionally, but operate in a single cell as a single biochemical cycle. Apart from that, the activation of this cycle in hepatocytes has deleterious consequences for liver function. Finally, we show that the application of mitochondrial-targeted antioxidant may interrupt this cycle and recover liver function. We anticipate our results to be the missing mechanistic link between acute systemic inflammation and liver failure.

mitochondria *via* mitochondrial permeability transition pore (15) and anion channels (32). Thus, both $O_2^{\bullet -}$ and H_2O_2 may contribute to intra- and extra-mitochondrial signaling. The initial event in ROS-mediated NO signaling may be the formation of peroxynitrite. Peroxynitrite was shown to cause tyrosine nitration, which impairs tyrosine phosphorylation (38), and has been suggested to interfere with kinase-mediated signaling pathways (21). Alternatively, NO regulates ROS production (5, 19), which, in turn, participates in intracellular signaling pathways *via* redox modification of SH groups by ROS (29). ROS have been shown to affect a number of other kinases and transcription factors, such as nuclear factor-κB (NF-κB) (45, 47, 49), hypoxia-inducible factor 1-alpha (20) or nuclear respiratory factor 2 (17), and signal transducers and activators of transcription (STAT) (35, 59) pathways operating on inflammation and upregulating a number of inflammatory genes such as inducible nitric oxide synthase (*iNOS*).

Although ROS have been suggested to regulate several signaling pathways, the origin of these ''regulatory'' ROS remains unclear and cannot be clearly attributed to specific subcellular ROS generators. Recent studies have highlighted the important role of mitochondrial ROS (mtROS) in the regulation of inflammation *via* activation of the inflammasome (60), stimulation of inflammatory cytokine production (3), and the modulation of innate immune responses by macrophages (58). It has recently been shown that mtROS are able to activate NOX (7, 8), suggesting that mitochondria generally regulate ROS production on inflammation.

Besides elevated ROS production, the inflammatory response is characterized by a drastic increase in NO levels due to upregulation of *iNOS* (40). NO itself exerts a multitude of effects on mitochondrial function, of which the inhibition of cytochrome oxidase is most dramatic regarding the energy supply for the cell (2). Furthermore, it is commonly accepted that a defect in mitochondrial function is causally involved in organ failure and particularly in liver failure (6, 51, 55).

The aim of this study was to clarify how the signaling network, comprising iNOS, mitochondria and ROS, influences liver function on systemic inflammation. The emphasis of this study was on the role of mtROS, assessed by analyzing the effects of mitochondria-targeted antioxidants (mtAOX) (13, 18, 43) in the liver.

Results

Selection of mtAOX concentrations

We tested mtAOX, mitoTEMPO, and SkQ1 (Fig. 1A, B), directed to mitochondria with alkyl-triphenyl-phosphonium-cation (52). To exclude a substantial inhibition of the electron transport chain (ETC) by mtAOX, we injected different doses of mitoTEMPO and SkQ1 into rats and determined respiratory function of mitochondria in liver homogenate. MitoTEMPO doses of 500 and 10,000 nmol/kg showed significantly decreased State 3 respiration with glutamate/malate in rat liver homogenates, whereas a dose of 50 nmol/kg showed only a declining trend (Fig. 1C). Doses of 50 or 500 nmol/kg of SkQ1 caused a decrease in State 3 respiration, while a dose of 5 nmol/kg showed no significant effect (Fig. 1D). We cannot exclude the fact that the trend of declining mitochondrial respiration occurring with 50 nmol/kg mitoTEMPO and 5 nmol/kg SkQ1 may reach significance with increased statistical power. However, this suggests, in our opinion, that at these concentrations there is a weak interaction between mtAOX and the ETC. We assume that this interaction may be beneficial for the recovery of the antioxidant capacity of the mtAOX molecules as previously suggested (1). Based on these data, we chose 50 nmol/kg mitoTEMPO and 5 nmol/kg SkQ1 for the *in vivo* experiments.

In the *in vitro* experiments, we used only mitoTEMPO due to its better solubility and accessibility for cultured cells. We tested the influence of different mitoTEMPO concentrations (Fig. 1E) on the mitochondrial membrane potential of hepatocytes. The highest concentration that did not cause membrane potential decrease was 0.5 μM, while for non-targeted TEMPO (Fig. 1F) this concentration was 100 times higher (compare Fig. 1E, F). Based on these data, we used 0.5 μM mitoTEMPO for the *in vitro* experiments.

Organ damage markers

The design of the *in vivo* experimental model is presented in Supplementary Figure S1 (Supplementary Data are available online at www.liebertpub.com/ars). We determined three markers of tissue damage: lactate dehydrogenase (LDH), aspartate aminotransferase (AST), and alanine aminotransferase (ALT). The levels of LDH, AST, and ALT rose between 2 (Fig. 2A–C) and 8 h in all lipopolysaccharide (LPS)-treated animals. While at 2 h only AST in the LPS + S group showed a significant increase (Fig. 2B), at 8 h some groups displayed a moderate but significant increase in the levels of LDH, AST, and ALT (Fig. 2D–F). A drastic increase of tissue damage markers occurred at 16 h after LPS challenge (Fig. 2G–I). In contrast, all animals pre-treated with mtAOX displayed similar values as the control (CO) animals except LDH levels in the LPS + S group (Fig. 2G). These findings suggest that treatment with mtAOX apparently has a tissue protective effect.

Histological examination

After 16 h (Supplementary Fig. S10), we observed moderate focal necrosis in animals receiving LPS, while 95% of the

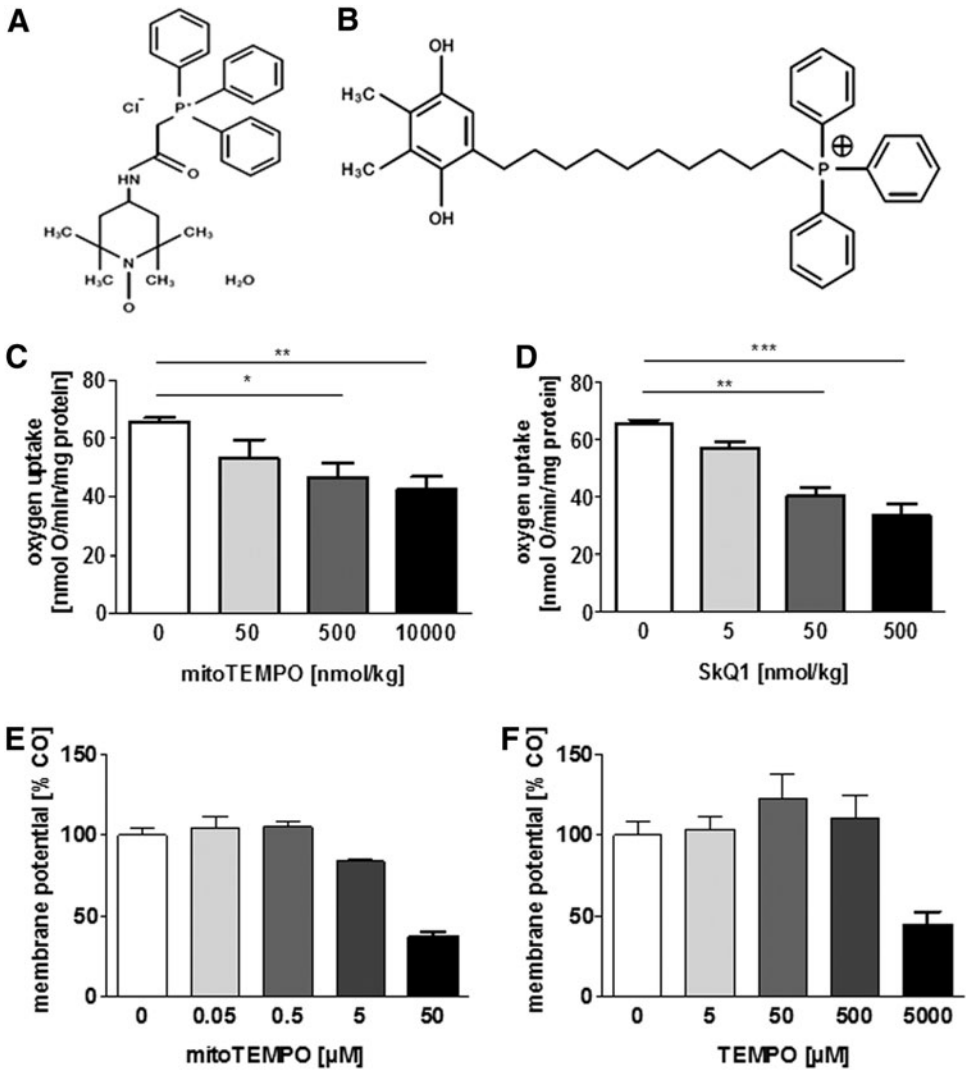

FIG. 1. Chemical structure and effect of mtAOX on mitochondria. Chemical structure of mitoTEMPO [(2-(2,2,6,6-tetramethylpiperidin-1-oxyl-4-ylamino)-2-oxoethyl)triphenylphosphonium chloride.monohydrate] and SkQ1 [10-(6′-plastoquinonyl) decyl-triphenyl-phosphonium] are displayed in **(A)** and **(B)**. **(C, D)** Show the effect of mtAOX on mitochondrial respiration in State 3 in liver homogenates obtained from animals receiving different doses of mitoTEMPO [**(C)**; 0, 50, 500, and 10,000 nmol/kg] or SkQ1 [**(D)**; 0, 5, 50, and 500 nmol/kg]. **(E, F)** Show effects of mitoTEMPO **(E)** and the non-targeted TEMPO **(F)** on the mitochondrial membrane potential in BLR3A cells. BLR3A cells were incubated with different concentrations of mtAOX mitoTEMPO (0, 0.05, 0.5, 5, and 50 μM) or non-targeted AOX TEMPO (0, 5, 50, 500, and 5000 μM). Membrane potential of mitochondria was detected by staining with MitoTracker Deep Red and is expressed as percentage of the corresponding control (CO) (0 μM). Data are expressed as mean ± SEM of $n = 6$ **(C, D)**, $n = 3$ **(E, F)**. $^{*}p < 0.05$, $^{**}p < 0.01$, $^{***}p < 0.001$. BRL3A, buffalo rat liver cell line-3A; CO, control; mtAOX, mitochondrial targeted antioxidants; SEM, standard error of the mean.

tissue appeared normal. CO animals as well as SkQ1 or mitoTEMPO-treated animals showed no formation of necrosis. (Supplementary Fig. S2C-E).

Mitochondrial function

We determined State 2 respiration (Fig. 3A, D, and G), reflecting the permeability of the inner mitochondrial membrane, and State 3 respiration with glutamate/malate (Fig. 3B, E, and H) and succinate (Fig. 3C, F, and I) reflecting ATP synthesis in liver homogenates. We did not see any significant difference either between LPS and CO or between LPS and groups treated with mtAOX. We observed a distinct trend to increasing State 3 respiration with glutamate/malate in the LPS group compared with COs and with groups treated with mtAOX (Fig. 3B, H). Moreover, we measured uncoupled oxidative phosphorylation with carbonyl cyanide *p*-trifluoro-methoxyphenyl hydrazine (Supplementary Fig. S2A, C, and E), and tested the intactness of the outer mitochondrial membrane with cytochrome c (Supplementary Fig. S2B, D, and F), but we did not find any significant differences between the groups.

Inflammatory/apoptosis markers in vivo

We determined expression of inflammatory markers, *iNOS*, interleukin *(IL)-6*, and tumor necrosis factor *(TNF)-alpha*, to characterize inflammatory response, as well as BCL2-associated X protein *(BAX)* and C/EBP homology protein

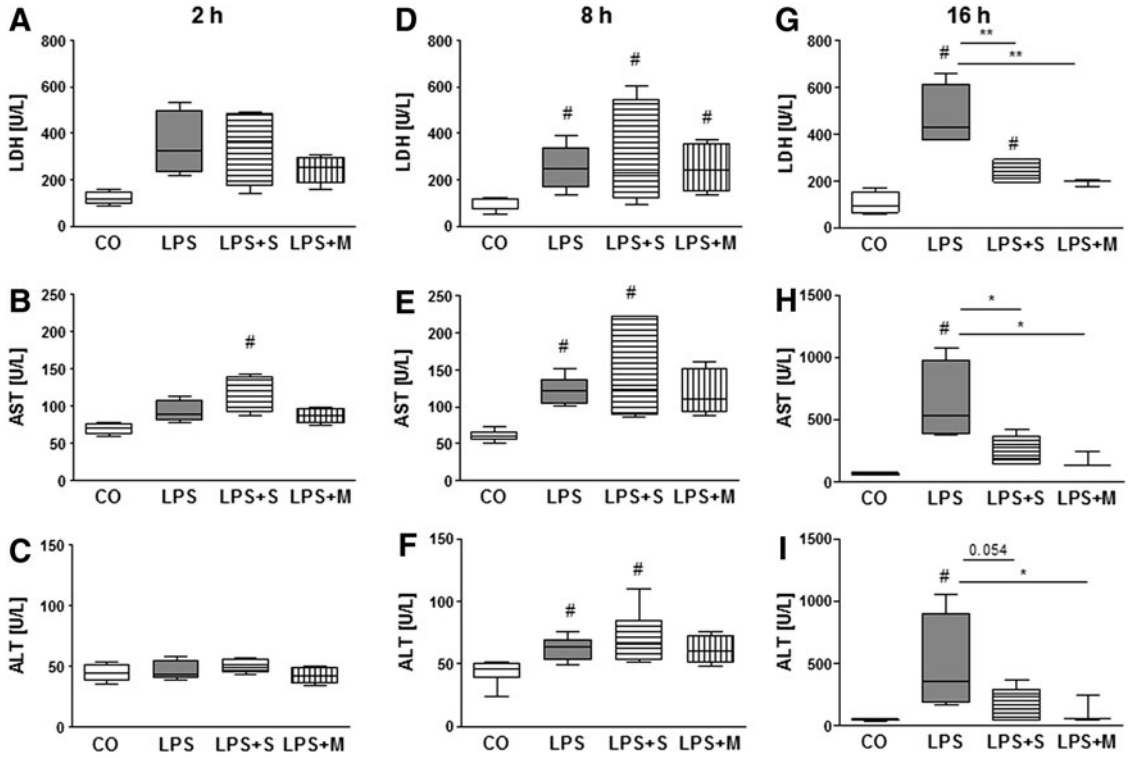

FIG. 2. Effect of systemic inflammatory response (SIR) and mtAOX *in vivo* on levels of organ damage markers. LPS (8 mg/kg) was injected intravenously into Sprague–Dawley rats. SkQ1 (S) or mitoTEMPO (M) (5 or 50 nmol/kg, respectively) was administered intraperitoneally at 24 and 1 h before LPS application (8 mg/kg). Saline was used for CO animals (no LPS application). Blood samples were harvested at 2 [$n=4$; **(A–C)**], 8 [$n=7$; **(D–F)**], or 16 h [$n=4$; **(G–I)**] after LPS application. Levels of tissue damage markers LDH **(A**, **D**, **G)**, AST **(B**, **E**, **H),** and ALT **(C**, **F**, **I)** were measured in plasma. $^{*}p<0.05$, $^{**}p<0.01$, $^{\#}p<0.05$ to control. ALT, alanine aminotransferase; AST, aspartate aminotransferase; LDH, lactate dehydrogenase; LPS, lipopolysaccharide; M, mitoTEMPO; S, SkQ1.

(CHOP) to characterize apoptosis at mRNA levels. In addition, we determined the expression of *NOX* to characterize non-mtROS sources. Two hours after onset of inflammation, the expression of *iNOS* (Fig. 4A), *IL-6* (Fig. 4B), and *TNF-alpha* (Supplementary Fig. S6A) was strongly increased in all three groups receiving LPS while the expression of *BAX* (Fig. 4C) did not change. In contrast, *CHOP* (Fig. 4D) was significantly downregulated in all groups receiving LPS. mtAOX did not influence *iNOS, IL-6*, or *TNF-alpha* levels after 2 h. At8 h, expression of *iNOS* (Fig. 4E), *IL-6* (Fig. 4F), and *TNF-alpha* (Supplementary Fig. S6B) decreased, but remained above CO values. *CHOP* and *BAX* were upregulated in all LPS-groups (Fig. 4G, H). mtAOX influenced neither levels of inflammatory markers nor markers of apoptosis at this time. Between 8 and 16 h, the levels of *iNOS* (Fig. 4I), *IL-6* (Fig. 4J), and *TNF-alpha* (Supplementary Fig. S6C) further decreased. In groups treated with mtAOX, the levels of *iNOS* (Fig. 4I) and *IL-6* (Fig. 4J) were significantly lower than in the non-treated LPS group while there were no differences of *TNF-alpha* levels in any of the LPS groups. TNF-alpha protein in blood (Supplementary Fig. S6D–F) reached its maximum level as early as at 2 h. This indicates that the upregulation of *TNF-alpha* mRNA occurs before upregulation of *iNOS* mRNA, confirming that TNF-alpha contributes to the induction of iNOS. The levels of apoptosis markers remained elevated at 16 h but were not affected by mtAOX treatment (Fig. 4K, L). *NOX* at mRNA level was upregulated in all LPS groups, but was not sensitive to mtAOX (Supplementary Fig. S8). These data suggest that mtAOX exert their beneficial effect *via* modulation of inflammatory response rather than *via* inhibition of cell death pathways.

NO generation

We detected NO-related signals in liver tissue and blood. In CO liver, we observed electron paramagnetic resonance (EPR) signals that were characteristic for liver tissue (Fig. 5A). The magnitude of the $g=2.25$ (cytochrome P450, Supplementary Fig. S3A, D, and G) and $g=1.93$ (predominantly succinate dehydrogenase, Supplementary Fig. S3C, F, and I) signals decreased in all LPS groups, while the magnitude of the $g=2.002$ (mitochondrial semiquinone/flavoproteins, Supplementary Fig. S3B, E, and H) signal was significantly elevated at 8 and 16 h. mtAOX did not strongly influence the magnitude of all three signals (Supplementary Fig. S3A–I). The strongest changes in the EPR spectra of liver were observed at $g=2.075$ and $g=2.042$, identified as mononitrosyl-hemoglobin-complexes (NO-Hb) formed in blood still remaining in the liver tissue and dinitrosyl iron complexes (NO-Fe) formed in liver cells (Fig. 5B). Both signals are predominantly present in liver tissue treated with nitrite (Fig. 5A, Li + NO). After 2 h, we did not observe significant changes in NO-Fe (Fig. 6A) and NO-Hb (Fig. 6B) levels in liver, while NO-Hb levels in blood were already significantly elevated (Fig. 6C). The highest NO-Hb levels in liver (Fig. 6E) and blood (Fig. 6F) were observed by 8 h simultaneously with *iNOS* expression in liver. In contrast, the levels of intracellular NO production (Fig. 6D) were slightly

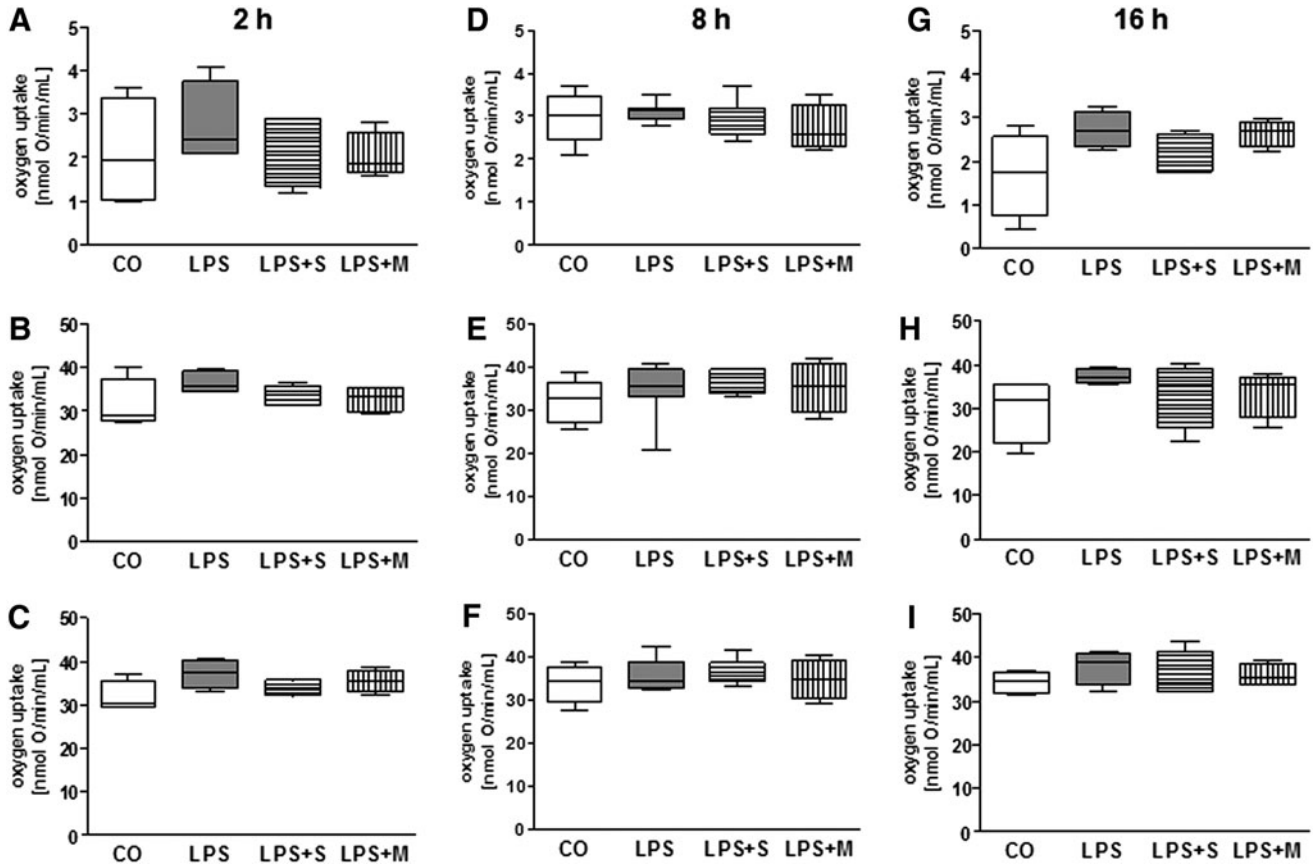

FIG. 3. Effect of SIR and mtAOX *in vivo* on respiratory function of liver mitochondria. Liver samples were harvested at 2 [$n=4$; **(A–C)**], 8 [$n=7$; **(D–F)**], or 16 h [$n=4$; **(G–I)**] after LPS application. Liver tissue was homogenized, and State 2 respiration of mitochondria was stimulated by addition of complex I substrates glutamate/malate [5 m*M*/5 m*M*; **(A**, **D**, **G)**] or complex II substrate succinate (10 m*M*) and complex I inhibitor rotenone (1 ng/ml; data not shown). Transition to complex I linked State 3 respiration of **(B**, **E**, **H)** and complex II linked State 3 respiration **(C**, **F**, **I)** was induced by addition of ADP (1 m*M*). ADP, adenosine diphosphate; M, mitoTEMPO; S, SkQ1.

increased in the LPS group. Between 8 and 16 h, the strongest changes were observed in NO-Fe levels (Fig. 6G), which were drastically increased in the LPS group and completely abolished by mtAOX. mtAOX significantly decreased NO-Hb levels in blood (Fig. 6I). This effect was even more pronounced for NO-Hb formed in vessels of liver tissue (Fig. 6H). Supplementary Figure S5A–D compares the time course of NO generation and *iNOS* expression after LPS challenge. The protein levels of iNOS reached a maximum at 8 h after LPS challenge and remained unchanged between 8 and 16 h (Supplementary Fig. S5E, F). At 8 h, the average value of iNOS protein was lower in the presence of SkQ1 (Supplementary Fig. S5G) but there was almost no effect of mtAOX at 16 h (Supplementary Fig. S5H). To better understand underlying intracellular mechanisms of interaction between mtAOX and NO synthesis in liver, we performed experiments with cultured hepatocytes *in vitro*.

Inflammatory response in hepatocytes

Inflammatory mediators (IMs) were generated by *ex vivo* incubation of white blood cells with LPS. Incubation of buffalo rat liver cells (buffalo rat liver cell line-3A [BRL3A]) with IM lead to an upregulation of *iNOS* at mRNA level at 1 h and further increased at 6 h (Fig. 7A). iNOS appeared at protein level after 6 h exposure to IM (Fig. 7B and Supplementary Fig. S9A). Laser scanning microscopy (LSM) imaging analysis (Fig. 7C) showed that elevated iNOS protein levels were accompanied by increased generation of NO in the cytosol of cells stimulated with IM (Fig. 7C[2], D). This increase in NO levels was accompanied by elevated generation of intracellular ROS. Figure 7E shows typical images of hepatocytes stained for mtROS and cytoplasmic ROS (cytROS). In CO cells (Fig. 7E[1–3]), only mtROS were detectable (Fig. 7E[1]), while the cytROS signal was below detection limit (Fig. 7E[2]). In contrast, in cells treated with IM, both mtROS (Fig. 7E[4]) and cytROS levels (Fig. 7E[5]) were elevated and cytROS were co-localized with mtROS (Fig. 7E[6]). cytROS were always detected in cytoplasmic areas that were associated with mitochondria (Fig. 7E[5]). Quantitative analysis of LSM images showed significantly elevated ROS levels in mitochondria (Fig. 7F) and cytoplasm (Fig. 7G) after 6 h of incubation with IM.

iNOS–ROS interaction in hepatocytes

MitoTEMPO strongly decreased expression of *iNOS* mRNA (Fig. 8A) and *IL-6* mRNA (Fig. 8B) but had a moderate effect on the NO level (Fig. 8C). L-Arginine caused an increase in NO levels in a concentration-dependent manner (Fig. 8D). In addition, mitoTEMPO reduced elevated levels of mtROS (Fig. 8E) and cytROS (Fig. 8F). L-NG-monomethyl arginine citrate

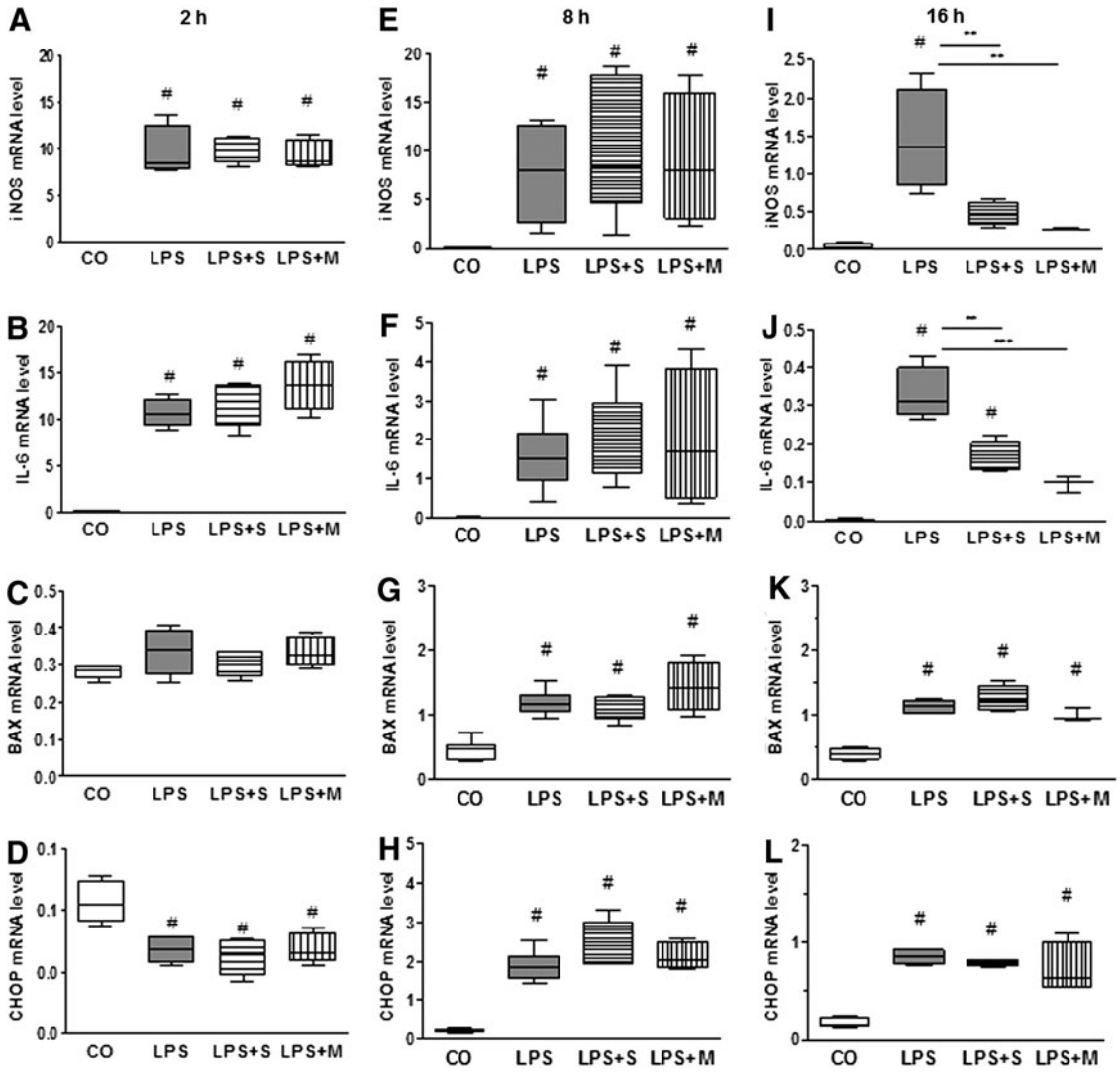

FIG. 4. Effect of SIR and mtAOX *in vivo* on gene expression of inflammatory and apoptosis markers. SkQ1 (S, 5 nmol/kg) or mitoTEMPO (M, 50 nmol/kg) were administered intraperitoneally at 24 and 1 h before LPS application (intravenously, 8 mg/kg). Saline was used for CO animals (no LPS application). Samples were taken at 2 [$n=4$; **(A–D)**], 8 [$n=7$; **(E–H)**], or 16 h [$n=4$; **(I–L)**] after the LPS application. RNA was isolated from snap-frozen liver tissue. Gene expression of the inflammatory markers *iNOS* **(A, E, I)** and *IL-6* **(B, F, J)**, and apoptosis markers *BAX* **(C, G, K)** and *CHOP* **(D, H, L)** was normalized using multiple reference genes (*HPRT*, *cyclophilin A*, and *GAPDH*). Data were calculated as $2^{-\Delta\Delta Cq}$ and are expressed relative to the internal standard, consisting of pooled aliquots of all investigated samples. $n \geq 4$. $^{**}p < 0.01$. $^{\#}p < 0.05$ to control. *BAX*, BCL2-associated X protein; *CHOP*, C/EBP homology protein; IL, interleukin; iNOS, inducible nitric oxide synthase; M, mitoTEMPO; S, SkQ1.

(L-NMMA), an inhibitor of NOS, was partially even more effective than mitoTEMPO. It decreased *IL-6* expression (Fig. 8B), abolished the increased NO levels elicited by IM (Fig. 8C), and decreased mtROS levels below original values (Fig. 8E). Treatment with 1400W dihydrochloride, a selective inhibitor of iNOS, decreased the average level of cytROS (Supplementary Fig. S7), but a more pronounced effect was observed in a combination of 1400W and mitoTEMPO.

Possible effect of endotoxin remaining in incubation medium

To test whether or not the LPS remaining in the medium after IM generation has an effect on the gene expression of iNOS and IL-6, we determined *iNOS* and *IL-6* mRNA levels in four CO groups. Both mRNA levels were detected in BRL3A cells without incubation (CO, 0 h) or after 6 h of incubation (CO, CO-conditioned medium [CM], CO + LPS, and IM). BRL3A cells were incubated with either cell culture medium (CO, 6 h) or cell culture medium containing LPS (CO + LPS) or white blood cell-derived IMs. In addition, cells were exposed to medium generated by *ex vivo* incubation of white blood cells (WBC) without LPS (CO-CM). Supplementary Figure S11 shows that incubation with CO-CM as well as CO + LPS elevated the levels of *iNOS* (Supplementary Fig. S11A) and *IL-6* mRNA (Supplementary Fig. S11B), but this elevation was ~1–2% compared with the effects of IM.

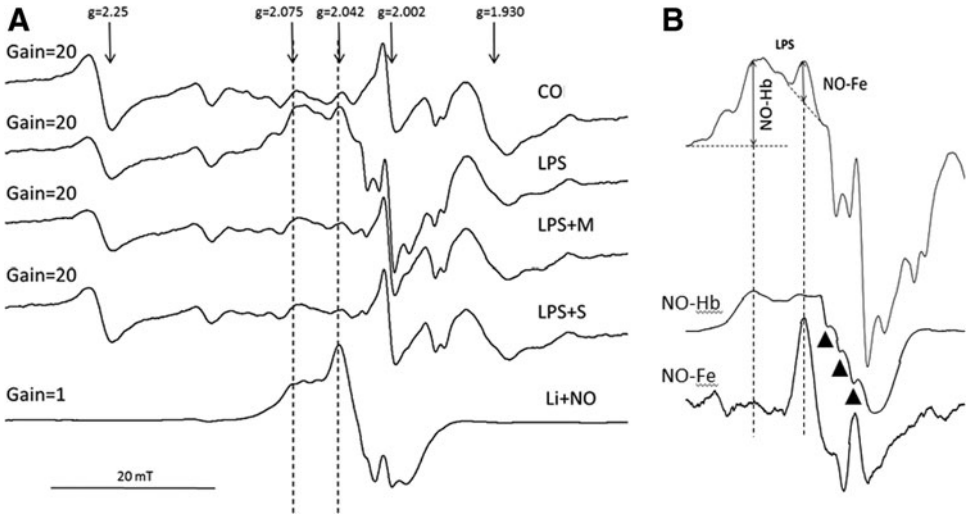

FIG. 5. Typical EPR spectra of NO detection in liver tissue (A) and detailed EPR spectra of NO-Hb and NO-Fe in liver (B) after application of saline (CO), LPS, and mitoTEMPO (M) or SkQ1 (S). Samples were taken at 16 h after LPS application. Spectra were recorded at liquid nitrogen temperature. The following signals were analyzed: cytochrome P450 ($g = 2.25$), NO-Hb formed in blood vessels of liver tissue ($g = 2.075$), NO-Fe ($g = 2.042$), mitochondrial semiquinone plus flavoproteins ($g = 2.002$), and the signal at $g = 1.93$ coming predominantly from succinate dehydrogenase. ▲ indicate triplet structure characteristic for five coordinated NO-Hb complexes **(B)**. EPR, electron paramagnetic resonance; Li + NO, liver tissue and nitric oxide; M, mitoTEMPO; NO, nitric oxide; NO-Fe, dinitrosyl iron complexes; NO-Hb, mononitrosyl-hemoglobin-complexes; S, SkQ1.

Discussion

To address the pathophysiological relevance of the interaction between NO and mtROS in NO-mediated signaling pathways on inflammation, we applied two mtAOX, SkQ1 and mitoTEMPO. The maximal concentrations of SkQ1 (5 nmol/kg) and mitoTEMPO (50 nmol/kg) not impairing mitochondrial respiration were selected for *in vivo* experiments. This 10-fold difference of concentrations is probably due to the fact that plastoquinone has a structure similar to ubiquinone (Fig. 1B) and may more efficiently interact with the ETC than mitoTEMPO. In the *in vitro* model, we applied mitoTEMPO. We selected the highest concentration of mitoTEMPO that did not remarkably influence membrane potential. This concentration (500 n*M*) was 10 times higher than the concentration of our *in vivo* experiments (50 nmol/kg). We assume that mitoTEMPO is more effectively transported into liver cells than in cultured hepatocytes. In addition, higher oxygen concentrations occurring in cell culture may facilitate ROS generation and a higher rate of mtAOX consumption, reducing the concentration of mtAOX interfering with ETC.

It is known that LPS challenge is accompanied by the release of cytoplasmic enzymes (LDH, AST, and ALT), which are typical markers of tissue damage. The kinetics of these markers showed two phases in our model. During the first phase (0–8 h), the increase in the levels of all tissue damage markers was moderate and not sensitive to the presence of mtAOX. During the second phase (8–16 h), levels of LDH, AST, and ALT strongly increased in LPS-treated animals. However, in animals pre-treated with SkQ1 or mitoTEMPO, significantly lower levels of these tissue damage markers were found (Fig. 2). These data were supported by histological examination of the liver. LPS induced focal necrosis in the liver, which was abolished by the application of mtAOX. Similar results were recently obtained in another model of acute inflammation. In this very severe model of acute inflammation, the authors reported a strong increase in ALT/AST as early as 5 h after LPS/peptidoglycan G challenge. mtAOX (MitoQ, MitoE) reduced ALT/AST changes. The authors demonstrated that in this model, induction of inflammatory response was accompanied by the impairment of mitochondrial function which was improved by mtAOX (30). In our model, we also determined respiratory function of mitochondria. However, we found neither impaired mitochondrial function nor effects of mtAOX. These data suggest that liver dysfunction on systemic inflammatory response is not induced by altered mitochondrial respiration. The State 3 respiration, corresponding to the mitochondrial capacity to synthetize ATP, even showed an upward trend. These findings are in line with several studies with experimental sepsis models and septic patients, which did not report pathological changes in respiratory function or morphology of mitochondria (24, 37, 56). Another possible mechanism of liver failure may be cell death *via* apoptosis and necrosis. We found significantly modulated levels of the pro-apoptotic markers *BAX* and *CHOP* after LPS treatment. After 2 h, *BAX* did not change and *CHOP* levels decreased. Later, at 8 and 16 h, the levels of both markers were elevated but not influenced by mtAOX. LPS challenge resulted in the occurrence of focal necrotic areas in the liver at 16 h. Such necrotic areas were not observed in animals treated with mtAOX. This suggests that beneficial effects of mtAOX are not linked to either respiratory function of mitochondria or apoptotic signaling, but they inhibit pathways causing necrosis. These data are supported by our finding that mtAOX reduce the release of LDH/AST/ALT, which are often associated with the induction of cell death and necrosis.

Rather different effects of mtAOX were obtained by studying the expression of inflammatory genes in the liver. In order to clarify the sequence of events and to gain insight into how mtAOX prevent cell damage, we determined the kinetics of the expression of *iNOS*, the major source of NO under inflammatory conditions, and *TNF-alpha* and *IL-6*, regulators

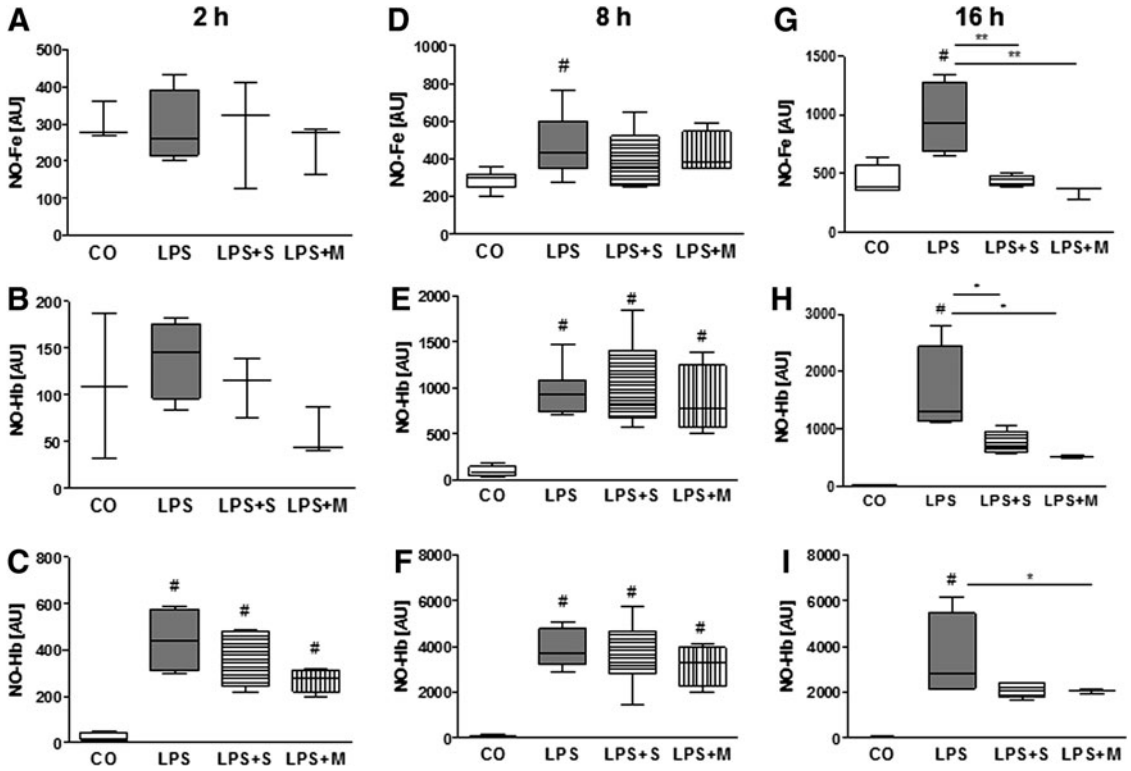

FIG. 6. Effect of SIR and mtAOX on NO generation in liver tissue and blood. Samples were taken at 2 [$n \geq 3$; **(A–C)**], 8 [$n = 7$; **(D–F)**], or 16 h [$n \geq 3$; **(G–I)**] after LPS application. Spectra were recorded at liquid nitrogen temperature. The peak magnitude was calculated for NO-Fe in liver **(A**, **D**, **G),** and the EPR spectra of NO-Hb in liver **(B**, **E**, **H)** or blood **(C**, **F**, **I)** were double integrated and expressed in AU. $^{*}p < 0.05$, $^{**}p < 0.01$. $^{\#}p < 0.05$ to control. AU, arbitrary units; M, mitoTEMPO; S, SkQ1.

of the acute phase response. As expected, we found a rapid increase in *TNF-alpha*, *IL-6*, and *iNOS* mRNA reaching the highest concentration at 2 h after LPS challenge. Later, the expression of these genes decreased, which is in line with previously published reports (12). Although the maximal expression of both *iNOS* and *IL-6* was determined in the first phase of acute inflammatory response (0–8 h), we saw neither a significant increase in the levels of cell damage markers nor any effects of mtAOX. This discrepancy can be explained by the fact that expression of *iNOS* and *IL-6* on mRNA level does not reflect the actual protein activity in the tissue. The activity of iNOS can be limited, for example, by the translational phase of expression, as well as by post-translational regulation, including the availability of substrates (L-arginine and oxygen). To address this issue with regard to the activity of iNOS, we determined the formation of NO in liver and blood using direct EPR detection in frozen tissues and NO oxidation products, nitrite and nitrate, in blood plasma. The strongest changes in the EPR spectra of the liver were observed in two EPR signals related to NO species. NO-Fe formed from NO produced within the cell (26) and NO-Hb originated from blood hemoglobin. The latter occurs in liver spectra due to blood remaining in liver vessels. Perfusion of liver does not influence NO-Fe level but leads to complete disappearance of the NO-Hb signal from the liver spectrum (data not shown). The signals of NO-Hb were increased in the blood as early as after 2 h; however, a more drastic increase was observed at 8 h. This strong increase of NO-Hb was clearly detectable in both blood and liver samples, while only small changes were observed in intracellular NO-Fe in the first phase of acute inflammation. This suggests that the NO formed in the first phase has originated from immune cells circulating in the blood, and from Kupffer cells rather than from hepatocytes. A rather different picture occurred during the second phase of inflammation. In the absence of mtAOX, blood-related NO-Hb signals did not change significantly, while the intracellular NO-Fe signals strongly increased. At this phase, both intracellular (NO-Fe) and extracellular (NO-Hb; NO_x, Supplementary Fig. S4A) NO levels were sensitive to mtAOX. Predominantly, this effect was seen in intracellular NO levels as determined by NO-Fe levels. This suggests that, during second phase of inflammatory response, NO is generated by intracellular sources of liver cells. To better illustrate the origin of NO generated in the *in vivo* model, we plotted the kinetics of NO-Hb in blood, NO-Hb in liver vessels, NO-Fe in liver, *iNOS* mRNA levels, and iNOS protein of the LPS group in an additional Supplementary Figure S5A–E. We observed that the maximal levels of *iNOS* mRNA (2 h) preceded the maximal levels of NO-Hb in blood and elevated levels of iNOS protein in the liver, both of which occurred simultaneously by 8 h after LPS injection, suggesting that this NO pool originated from immune cells circulating in the blood and Kupffer cells predominantly located in small vessels. This is supported by the fact that intracellular NO concentrations determined by the formation of NO-Fe increased by 16 h. Intracellular levels of NO but not iNOS protein in the liver were sensitive to mtAOX, suggesting that iNOS protein predominantly is not hepatocyte derived. Furthermore, small changes of iNOS protein in hepatocytes would pass unnoticed compared with high levels of

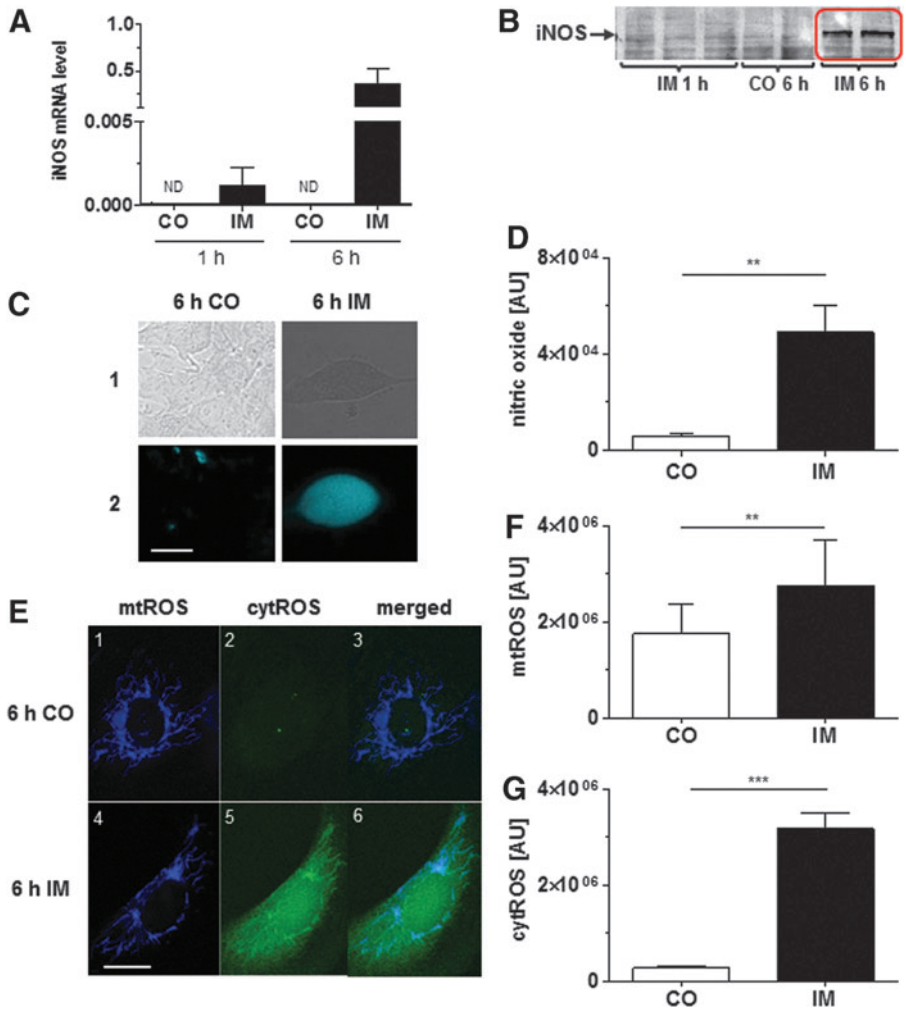

FIG. 7. Effect of IMs *in vitro* on *iNOS* expression, NO production (A–D), and ROS generation (E–G). BRL3A cells were incubated in cell culture medium (RPMI medium) without (CO) or with IMs **(A–G)**. Samples for polymerase chain reaction **(A)** and Western blot analysis **(B)** were collected at 1 and 6 h of incubation. LSM images **(C–G)** were taken at 6 h of incubation. **(C, E)** Scale bar representing 20 μm, magnification 630×. Cell images under phase-contrast microscopy **(C1)**. NO [*intense blue* color, **(C2)**] was stained with DAF-FM diacetate (ex/em 488/505 nm). mtROS [*deep blue* color; **(E, F)**] were stained with CM-H2XROS (ex/em 543/585 nm). cytROS [*green* color; **(E, G)**] were detected using 2′,7′-dichlorofluorescin diacetate (DCF-DA) (ex/em: 488/505 nm). LSM images of control cells **(E1-3)** and cells treated with IM **(E4-6)**. Gene expression of *iNOS* **(A)** was normalized using multiple reference genes (*HPRT*, *cyclophilin A*, and *GAPDH*). Data were calculated as $2^{-\Delta\Delta Cq}$ and are expressed relative to the internal standard, consisting of pooled aliquots of all investigated samples. Data are expressed as mean ± SEM of $n = 6$. $^{**}p < 0.01$, $^{***}p < 0.001$. cytROS, cytoplasmic reactive oxygen species; IM, inflammatory mediator; LSM, laser scanning microscopy; mtROS, mitochondrial reactive oxygen species; ND, not detectable; ROS, reactive oxygen species. To see this illustration in color, the reader is referred to the web version of this article at www.liebertpub.com/ars

non-hepatocyte iNOS protein. The maximal expression of *iNOS* and *IL-6* observed at 2 h was not accompanied by any pronounced increase in tissue damage markers and was not sensitive to mtAOX. These findings suggest that the initial pathway upregulating *iNOS* and *IL-6* gene expression and excessive NO generation is not ROS dependent.

However, during the second phase (8–16 h), most of the investigated parameters were modulated by mtAOX, suggesting that excessive ROS formation in mitochondria starts later. Pre-treatment with mtAOX accelerated the decay of *iNOS* expression, abolished excessive NO generation in liver and blood, and reduced organ damage occurring during this phase. The fact that mtAOX can reduce inflammation-mediated NO generation in the blood is in line with a recent publication by Plotnikov *et al.* (43). Our data indicate that acute inflammation induces at least two different mechanisms upregulating inflammatory genes. The first mechanism occurs earlier, is not ROS dependent, and does not induce organ dysfunction. The second occurs later when the expression of *iNOS* (and *IL-6*) has already passed the highest expression levels and returns to CO levels. Thus, organ damage occurs in an NO/mtROS-dependent manner. The changes in ALT/AST suggest that this mechanism operates in the liver, while elevated LDH levels may be a sign of damage to other organs. Although mtAOX target mitochondria, their beneficial effects are due to protection of the integrity of the cytoplasmic membrane and the release of cytoplasmic enzymes, rather than due to amelioration of mitochondrial dysfunction. Thus, our *in vivo* data suggest that the damage to cytoplasmic membranes occurs when NO and mtROS are generated simultaneously. This suggests the involvement of peroxynitrite, which has already been shown to directly damage cytoplasmic membrane *via* activated oxidative stress (46). Previously, we showed that LPS challenge increases ROS/peroxynitrite levels in the liver and several other organs (25). This is in line with previously reported data showing that hepatic mitochondria isolated from LPS-treated rats generate more mtROS preferentially by complex I (24, 25), and finally that these mitochondria leak mtROS (42). These findings suggest that mitochondria are the source of elevated ROS, a hallmark of the cellular response to inflammation. However, our *in vivo* experiments do not answer the question whether or not mtROS and NO are a part of the same pathologic process. If so, what is the nature of this process?

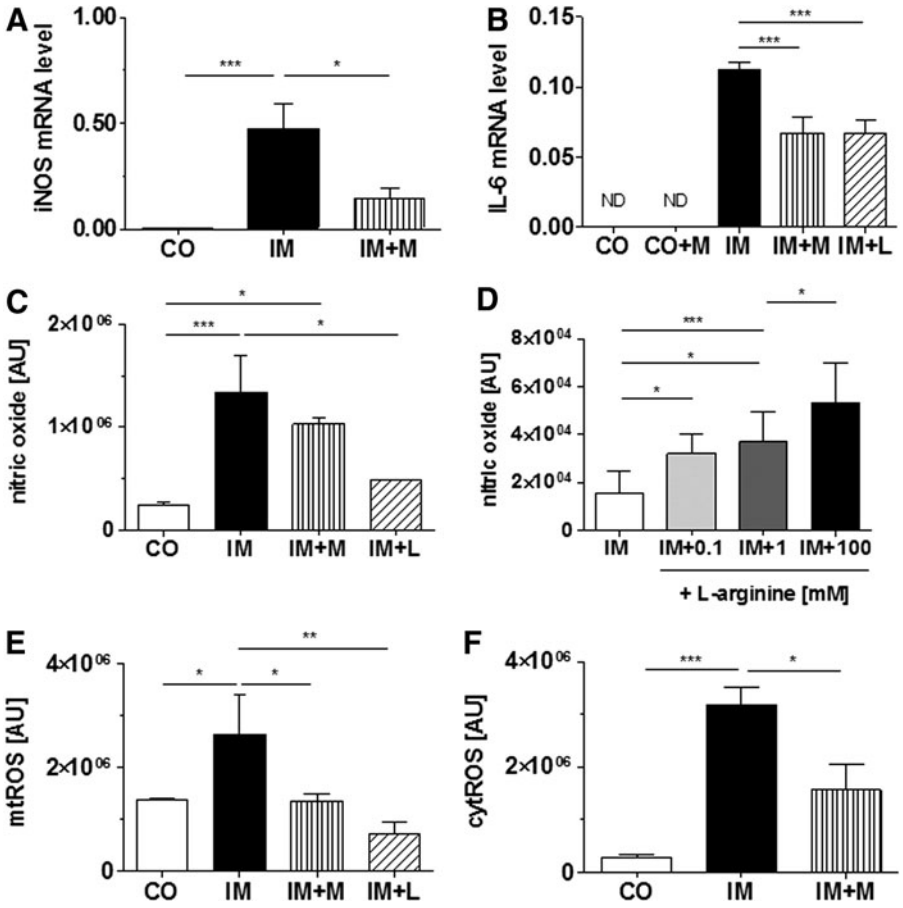

FIG. 8. Effect of *in vitro* treatment with ROS scavenger mitoTEMPO (M) or NOS inhibitor L-NMMA (L) on iNOS (A), IL-6 (B), NO (C) and ROS production (E, F), and effect of different doses of L-arginine on NO levels (D). BRL3A cells were incubated in cell culture medium (RPMI1640) without (CO) or with IMs, with or without ROS scavenger mitoTEMPO (M) or NOS inhibitor L-NMMA (L). Samples were taken at 6 h. For LSM investigation, cells were stained with fluorescent dyes for detection of mtROS (CM-H2XROS, ex/em 543/585 nm) or cytROS (DCF-DA, ex/em: 488/505 nm). NO level was quantified with LSM imaging (DAF-FM diacetate, ex/em 488/505 nm). Gene expression of *iNOS* **(A)** and *IL-6* **(B)** was normalized using multiple reference genes (*HPRT*, *cyclophilin A*, and *GAPDH*). Data were calculated as $2^{-\Delta\Delta Cq}$ and are expressed relative to the internal standard, consisting of pooled aliquots of all investigated samples. Data are expressed as mean ± SEM of at least $n \geq 3$. $^{*}p < 0.05$, $^{**}p < 0.01$, $^{***}p < 0.001$. L-NMMA, L-NG-monomethyl arginine citrate; M, mitoTEMPO; ND, not detectable.

Serious limitations of an *in vivo* model do not allow further investigations of intracellular interactions between NO and mtROS. Inhibition of NO synthesis affects not only intracellular but also systemic processes. It has been shown that inhibition of NOS aggravates organ failure, likely due to hemodynamic effects of NO (36). Our data show that there are two mechanisms upregulating NO levels, but only one of these causes tissue damage. *In vivo,* it is impossible to detect mtROS separately from other intracellular and extracellular ROS and it is difficult to assess interactions between NO formed by iNOS in cytoplasm and mtROS generated in mitochondria. Furthermore, liver failure is linked to hepatocytes and liver, but the cell population extracted in *in vivo* models contains different cell types. Therefore, the effects described earlier can be attributed to other than hepatocyte cell types. These disadvantages of the *in vivo* model can be excluded by experiments with specific cell types. We, therefore, used a hepatocyte culture model to separately determine the generation of non-mitochondrial cytROS, mtROS, as well as intracellular NO levels.

Recently, we described such a model based on the generation of IM by incubation of WBC with LPS, simulating the immune response in an *in vivo* model. To ensure that possible effects observed after incubation with generated IM are not due to the LPS remaining in the medium, we performed CO experiments (Supplementary Fig. S11) showing that the presence of LPS in medium caused an elevation of *iNOS* and *IL-6* mRNA levels of 1–2% compared with the effects of IM. In this study, we incubated hepatocytes (BRL3A cell line) with generated IM and determined the time course of *iNOS* expression. After 1 h of incubation with IM, an upregulation of *iNOS* mRNA was observed, further increasing to 6 h. Elevated levels of iNOS protein and NO were detected at 6 h, with the latter found in the cytoplasm. These data suggest that iNOS is the major NO source in the cytoplasm and probably in other subcellular organelles. To analyze the generation of intracellular ROS, we used a combination of two fluorescent dyes, CM-H2XROS and DCF-DA. This allowed access to both mtROS and cytROS. In CO cells, we found low levels of mtROS and even less cytROS. Treatment with IM caused an increase of both mtROS and, even more so, cytROS. Interestingly, cytROS were found to be co-localized with mtROS. Moreover, the highest cytROS levels were found in close vicinity to mitochondria, suggesting that mtROS diffuse into the cytoplasm, which is in line with previous reports (42). mtROS may contribute to intracellular signaling either directly, diffusing in cytoplasm, or indirectly *via* amplification by other intracellular ROS sources. Several recent publications demonstrated that mtROS can activate NOX in immune cells (7). Depletion of mitochondrial superoxide dismutase (mtSOD) and opening of mitochondrial permeability transition pore activate this signaling pathway (27). mtROS-dependent activation of NOX is mediated by Ca^{2+} release, which turns on protein kinase C-dependent activation of phagocytic NOX (9). Moreover, it has recently been suggested that mtROS orchestrate not only NOX but also other intracellular sources of ROS, such as XOR (50). The occurrence of cross-talk between mtROS and NOX has also been

shown in non-immune endothelial cells on an interaction with angiotensin II. In this model, similar to our study, elevated ROS formation was accompanied by an increase in NO levels. The deleterious effect of excessive ROS/NO formation was associated with the formation of $ONOO^-$ (11). Overexpression of mtSOD abolished deleterious NOX-mediated effects of angiotensin (10), suggesting that $O_2^{\bullet -}$ and not H_2O_2 contributes to mitochondrial signaling, as SOD increases H_2O_2 generation from $O_2^{\bullet -}$. They suggest that $ONOO^-$ is the major damaging agent, escaping this signaling pathway; this is in line with the interpretation of our data (Supplementary Fig. S12). Since elevated levels of cytROS and NO occurred simultaneously in our model, we examined the interaction between NO and ROS. We tested the effects of mitoTEMPO and L-NMMA, an inhibitor of NO synthase. MitoTEMPO abolished not only the increase in mtROS levels induced by IMs but also the levels of cytROS. This again can be explained by the diffusion of mtROS into the cytoplasm. L-NMMA also decreased mtROS levels and was even more efficient than mitoTEMPO, suggesting that NO induces mtROS production. We observed that mitoTEMPO downregulated expression of *iNOS* and *IL-6* and reduced NO levels. The effect of mitoTEMPO on *iNOS* expression was stronger than on NO levels, suggesting that NO generation was limited not only by the amount of iNOS enzyme *per se* but also by levels of L-arginine, the substrate of iNOS. This may explain the weak effect of mitoTEMPO on NO generation. Indeed, the addition of L-arginine to cultured hepatocytes strongly increased NO levels, suggesting that the concentration of L-arginine limits the activity of NOS. Similar data were previously obtained *in vivo*, showing that the infusion of L-arginine in rats increases the level of circulating NO-Hb (23). Since insufficient concentrations of L-arginine may result in the generation of $O_2^{\bullet -}$ by NOS, we cannot exclude that $O_2^{\bullet -}$ may also contribute to the iNOS-mtROS cycle [Reviewed in ref. (31)]. Irrespective of which species is involved in the iNOS-mediated signaling, our results suggest that mitoTEMPO downregulates iNOS at transcriptional level *via* an mtROS-dependent pathway. We assume that this pathway is activated when mtROS diffuse out of the mitochondria and interact with transcriptional factors such as NF-κB, STAT, or other ROS-dependent pathways, provoking an inflammatory response program. Our *in vitro* data strongly suggest a feed-forward loop (iNOS-mtROS cycle, Supplementary Fig. S12) regulating mtROS production and iNOS expression. The existence of this cycle satisfactorily explains the data obtained *in vivo*, confirming that this loop induces tissue damage. Scavenging mtROS prevents this damage as indicated by decreased plasma levels of LDH, a marker of tissue damage not directly related to specific organs. This occurs to a higher degree than for AST and ALT, which are liver-specific markers. Thus, our data suggest that the iNOS-mtROS loop is a vicious cycle which accelerates the damaging effect of IM in the liver and probably in other tissues. Further studies are required to identify intracellular signaling pathways activating the iNOS-mtROS cycle.

Materials and Methods

Chemicals

All reagents were obtained from Sigma-Aldrich unless otherwise noted.

Animals

Adult male Sprague–Dawley rats (250–300 g) were purchased from the Animal Research Laboratories. All animal procedures were approved by the Local Legislative Committee and conducted according to the National Institute of Health Guidelines.

Design of animal experiment

Previously, we performed a pilot study to select the appropriate range of mtAOX concentrations for the *in vivo* study. In this study (Supplementary Fig. S1), adult male Sprague–Dawley rats were injected intravenously (*vena dorsalis penis*) with LPS (*Escherichia coli* Serotype 026:B6; 8 mg/kg). Treatment with the mtAOX SkQ1 (5 nmol/kg = 3.1 μg/kg) and mitoTEMPO (50 nmol/kg = 25.5 μg/kg) was administered intraperitoneally. Samples were taken at 2, 8, or 16 h after LPS application. For detailed information, see Supplementary Methods.

Design of cell culture experiment

We chose the dose of mitoTEMPO based on a pilot study. In this study, BRL3A cells were incubated with cell culture medium (RPMI1640) or CM (RPMI1640 containing IMs) and treated with L-NMMA (10 n*M*), 1400W dihydrochloride (5 μ*M*), mitoTEMPO (500 n*M*), or L-arginine. For further details, see Supplementary Methods.

WBC isolation and generation of CM

IMs were produced as previously described (57). For further details, see Supplementary Methods.

Enzyme assays

AST, ALT, and LDH were analyzed in plasma using a Cobas c 111 reader (Roche). Samples were taken at different time points as indicated in figure legends.

Histological examination

Liver tissues were fixed in 4% formaldehyde solution buffered with phosphate for 24 h and embedded in paraffin. Tissue sections were stained with hematoxylin and eosin and examined by light microscopy.

Laser scanning microscopy

For confocal microscopic investigations, cells were stained with fluorescent dyes for detection of mtROS, cytROS, and oxidative products of NO. Imaging was performed with an inverted confocal microscope (LSM 510; Zeiss). For further details, see Supplementary Methods.

Western blot analysis

Western blots of washed cell pellets dissolved in Laemmli buffer or of appropriately diluted liver homogenates were performed as previously described (37, 44). For further details, see Supplementary Methods.

Determination of nitrosylated hemoglobin (NO-Hb) in blood samples

Whole blood was centrifuged and red blood cells, placed in 1 ml syringes (Omnifix, U-100 Insulin; Braun), were frozen.

EPR spectra (Supplementary Fig. S4B) were recorded at liquid nitrogen temperature (−196°C) with a Magnettech MiniScope MS 200 EPR spectrometer (Magnettech Ltd.). The general settings were as follows: modulation frequency 100 kHz, microwave frequency 9.425 GHz, microwave power 8.3 mW, modulation amplitude 5 G, and gain 200. NO-Hb were recorded at 3300 ± 200 G and quantified by double integrating the EPR spectra.

Determination of nitrosylated hemoglobin (NO-Hb) and NO-Fe in liver samples

Liver samples were placed in 1 ml syringes (Omnifix, U-100 Insulin; Braun) and frozen. The EPR spectra from frozen samples were recorded in a Miniscope MS 200 EPR spectrometer (Magnettech Ltd.) at liquid nitrogen temperature with the following settings: modulation frequency 100 kHz, microwave frequency 9.429 GHz, microwave power 30 mW, and modulation amplitude 6 G. Liver spectra were recorded at 3200 ± 500 G.

Analysis of total NO

Total NO levels (NO_x) were analyzed with Sievers 280i-NO Analyzer (General Electrics) as previously reviewed in Pelletier *et al*. (41). Plasma samples were injected through a septum into the glass vessel, where NO species were converted by a redox active reagent (VCl_3) to $NO_{(g)}$. A subsequent reaction with O_3 caused photon emission, which was detected as chemiluminescence.

Mitochondrial respiration

Respiratory parameters of mitochondria were monitored using a high-resolution respirometer (Oxygraph-2k; Oroboros Instruments). For details, see Supplementary Material.

cDNA synthesis and quantitative polymerase chain reaction

RNA was extracted from rat liver samples or BRL3A cells using TriReagent™ in accordance to the manufacturer's protocol. Reverse transcription, quantitative polymerase chain reaction, and data processing were performed as previously described (22, 28, 57). Specific primer pairs are shown in Supplementary Table S2. For detailed information, see Supplementary material.

Flow cytometric immunoassay

The concentration of TNF-alpha in the plasma was detected with Rat Basic Kit FlowCytomix™ (eBioscience) according to the manufacturer's manual.

Statistical analysis

Statistical analysis of data was performed by one-way analysis of variance followed by Tukey *post hoc* test in normally distributed data and Kruskal–Wallis combined with Mann–Whitney test in groups showing a non-Gaussian distribution. Taking into account that the data *in vivo* were partially not normally distributed, we presented the data as box plots. In contrast, *in vitro* data were normally distributed and presented as mean ± standard error of the mean. Calculations were performed using GraphPad Prism (GraphPad Software) and SPSS 15 software (SPSS, Inc.). The number of independent samples (n) is indicated in figure legends. The significance level was set at 0.05 and is indicated as $^{*}p < 0.05$, $^{**}p < 0.01$, $^{***}p < 0.001$, and $^{\#}p < 0.05$ to CO.

Acknowledgments

The authors thank Ingeborg Kehrer for establishing the *in vitro* model of inflammation; Sergiu Dumitrescu, Martin Perlinger, Stefan Puchner, Mohammad Jafarmadar, and Christine Kober for their excellent technical assistance; Carina Penzenstadler and Claudia Keibl for assistance with the animal experiment; and Carina Wagner and James Ferguson for assistance in the preparation of this article. A.W. was supported by FFG (Austria, COMET K-Project 825329, BioPersMed).

Author Disclosure Statement

No competing financial interests exist.

References

1. Antonenko YN, Avetisyan AV, Bakeeva LE, Chernyak BV, Chertkov VA, Domnina LV, Ivanova OY, Izyumov DS, Khailova LS, Klishin SS, Korshunova GA, Lyamzaev KG, Muntyan MS, Nepryakhina OK, Pashkovskaya AA, Pletjushkina OY, Pustovidko AV, Roginsky VA, Rokitskaya TI, Ruuge EK, Saprunova VB, Severina II, Simonyan RA, Skulachev IV, Skulachev MV, Sumbatyan NV, Sviryaeva IV, Tashlitsky VN, Vassiliev JM, Vyssokikh MY, Yaguzhinsky LS, Zamyatnin AA, Jr., and Skulachev VP. Mitochondria-targeted plastoquinone derivatives as tools to interrupt execution of the aging program. 1. Cationic plastoquinone derivatives: synthesis and *in vitro* studies. *Biochemistry (Mosc)* 73: 1273–1287, 2008.
2. Brown GC. Nitric oxide regulates mitochondrial respiration and cell functions by inhibiting cytochrome oxidase. *FEBS Lett* 369: 136–139, 1995.
3. Bulua AC, Simon A, Maddipati R, Pelletier M, Park H, Kim KY, Sack MN, Kastner DL, and Siegel RM. Mitochondrial reactive oxygen species promote production of proinflammatory cytokines and are elevated in TNFR1-associated periodic syndrome (TRAPS). *J Exp Med* 208: 519–533, 2011.
4. Chen CA, Wang TY, Varadharaj S, Reyes LA, Hemann C, Talukder MA, Chen YR, Druhan LJ, and Zweier JL. S-glutathionylation uncouples eNOS and regulates its cellular and vascular function. *Nature* 468: 1115–1118, 2010.
5. Chouchani ET, Methner C, Nadtochiy SM, Logan A, Pell VR, Ding S, James AM, Cocheme HM, Reinhold J, Lilley KS, Partridge L, Fearnley IM, Robinson AJ, Hartley RC, Smith RA, Krieg T, Brookes PS, and Murphy MP. Cardioprotection by S-nitrosation of a cysteine switch on mitochondrial complex I. *Nat Med* 19: 753–759, 2013.
6. Crouser ED, Julian MW, Blaho DV, and Pfeiffer DR. Endotoxin-induced mitochondrial damage correlates with impaired respiratory activity. *Crit Care Med* 30: 276–284, 2002.
7. Daiber A. Redox signaling (cross-talk) from and to mitochondria involves mitochondrial pores and reactive oxygen species. *Biochim Biophys Acta* 1797: 897–906, 2010.
8. Dikalov S. Cross talk between mitochondria and NADPH oxidases. *Free Radic Biol Med* 51: 1289–1301, 2011.

9. Dikalov SI, Li W, Doughan AK, Blanco RR, and Zafari AM. Mitochondrial reactive oxygen species and calcium uptake regulate activation of phagocytic NADPH oxidase. *Am J Physiol Regul Integr Comp Physiol* 302: R1134–R1142, 2012.
10. Dikalova AE, Bikineyeva AT, Budzyn K, Nazarewicz RR, McCann L, Lewis W, Harrison DG, and Dikalov SI. Therapeutic targeting of mitochondrial superoxide in hypertension. *Circ Res* 107: 106–116, 2010.
11. Doughan AK, Harrison DG, and Dikalov SI. Molecular mechanisms of angiotensin II-mediated mitochondrial dysfunction: linking mitochondrial oxidative damage and vascular endothelial dysfunction. *Circ Res* 102: 488–496, 2008.
12. Duvigneau JC, Piskernik C, Haindl S, Kloesch B, Hartl RT, Huttemann M, Lee I, Ebel T, Moldzio R, Gemeiner M, Redl H, and Kozlov AV. A novel endotoxin-induced pathway: upregulation of heme oxygenase 1, accumulation of free iron, and free iron-mediated mitochondrial dysfunction. *Lab Invest* 88: 70–77, 2008.
13. Fink MP, Macias CA, Xiao J, Tyurina YY, Jiang J, Belikova N, Delude RL, Greenberger JS, Kagan VE, and Wipf P. Hemigramicidin-TEMPO conjugates: novel mitochondria-targeted anti-oxidants. *Biochem Pharmacol* 74: 801–809, 2007.
14. Hino K, Hara Y, and Nishina S. Mitochondrial reactive oxygen species as a mystery voice in hepatitis C. *Hepatol Res* 44: 123–132, 2014.
15. Hou Y, Ghosh P, Wan R, Ouyang X, Cheng H, Mattson MP, and Cheng A. Permeability transition pore-mediated mitochondrial superoxide flashes mediate an early inhibitory effect of amyloid beta1-42 on neural progenitor cell proliferation. *Neurobiol Aging* 35: 975–989, 2014.
16. Ito N, Ruegg UT, Kudo A, Miyagoe-Suzuki Y, and Takeda S. Activation of calcium signaling through Trpv1 by nNOS and peroxynitrite as a key trigger of skeletal muscle hypertrophy. *Nat Med* 19: 101–106, 2013.
17. Itoh K, Tong KI, and Yamamoto M. Molecular mechanism activating Nrf2-Keap1 pathway in regulation of adaptive response to electrophiles. *Free Radic Biol Med* 36: 1208–1213, 2004.
18. James AM, Cocheme HM, Smith RA, and Murphy MP. Interactions of mitochondria-targeted and untargeted ubiquinones with the mitochondrial respiratory chain and reactive oxygen species. Implications for the use of exogenous ubiquinones as therapies and experimental tools. *J Biol Chem* 280: 21295–21312, 2005.
19. Juhaszova M, Zorov DB, Kim SH, Pepe S, Fu Q, Fishbein KW, Ziman BD, Wang S, Ytrehus K, Antos CL, Olson EN, and Sollott SJ. Glycogen synthase kinase-3beta mediates convergence of protection signaling to inhibit the mitochondrial permeability transition pore. *J Clin Invest* 113: 1535–1549, 2004.
20. Kietzmann T and Gorlach A. Reactive oxygen species in the control of hypoxia-inducible factor-mediated gene expression. *Semin Cell Dev Biol* 16: 474–486, 2005.
21. Kong SK, Yim MB, Stadtman ER, and Chock PB. Peroxynitrite disables the tyrosine phosphorylation regulatory mechanism: lymphocyte-specific tyrosine kinase fails to phosphorylate nitrated cdc2(6–20)NH2 peptide. *Proc Natl Acad Sci U S A* 93: 3377–3382, 1996.
22. Kozlov AV, Duvigneau JC, Miller I, Nurnberger S, Gesslbauer B, Kungl A, Ohlinger W, Hartl RT, Gille L, Staniek K, Gregor W, Haindl S, and Redl H. Endotoxin causes functional endoplasmic reticulum failure, possibly mediated by mitochondria. *Biochim Biophys Acta* 1792: 521–530, 2009.
23. Kozlov AV, Sobhian B, Costantino G, Nohl H, Redl H, and Bahrami S. Experimental evidence suggesting that nitric oxide diffuses from tissue into blood but not from blood into tissue. *Biochim Biophys Acta* 1536: 177–184, 2001.
24. Kozlov AV, Staniek K, Haindl S, Piskernik C, Ohlinger W, Gille L, Nohl H, Bahrami S, and Redl H. Different effects of endotoxic shock on the respiratory function of liver and heart mitochondria in rats. *Am J Physiol Gastrointest Liver Physiol* 290: G543–G549, 2006.
25. Kozlov AV, Szalay L, Umar F, Fink B, Kropik K, Nohl H, Redl H, and Bahrami S. Epr analysis reveals three tissues responding to endotoxin by increased formation of reactive oxygen and nitrogen species. *Free Radic Biol Med* 34: 1555–1562, 2003.
26. Kozlov AV, Yegorov DY, Vladimirov YA, and Azizova OA. Intracellular free iron in liver tissue and liver homogenate: studies with electron paramagnetic resonance on the formation of paramagnetic complexes with desferal and nitric oxide. *Free Radic Biol Med* 13: 9–16, 1992.
27. Kroller-Schon S, Steven S, Kossmann S, Scholz A, Daub S, Oelze M, Xia N, Hausding M, Mikhed Y, Zinssius E, Mader M, Stamm P, Treiber N, Scharffetter-Kochanek K, Li H, Schulz E, Wenzel P, Munzel T, and Daiber A. Molecular mechanisms of the crosstalk between mitochondria and NADPH oxidase through reactive oxygen species-studies in white blood cells and in animal models. *Antioxid Redox Signal* 20: 247–266, 2014.
28. Kyto V, Lapatto R, Lakkisto P, Saraste A, Voipio-Pulkki LM, Vuorinen T, and Pulkki K. Glutathione depletion and cardiomyocyte apoptosis in viral myocarditis. *Eur J Clin Invest* 34: 167–175, 2004.
29. Liu H, Colavitti R, Rovira II, and Finkel T. Redox-dependent transcriptional regulation. *Circ Res* 97: 967–974, 2005.
30. Lowes DA, Webster NR, Murphy MP, and Galley HF. Antioxidants that protect mitochondria reduce interleukin-6 and oxidative stress, improve mitochondrial function, and reduce biochemical markers of organ dysfunction in a rat model of acute sepsis. *Br J Anaesth* 110: 472–480, 2013.
31. Luo S, Lei H, Qin H, and Xia Y. Molecular mechanisms of endothelial NO synthase uncoupling. *Curr Pharm Des* 20: 3548–3553, 2014.
32. Lustgarten MS, Bhattacharya A, Muller FL, Jang YC, Shimizu T, Shirasawa T, Richardson A, and Van RH. Complex I generated, mitochondrial matrix-directed superoxide is released from the mitochondria through voltage dependent anion channels. *Biochem Biophys Res Commun* 422: 515–521, 2012.
33. Meneshian A and Bulkley GB. The physiology of endothelial xanthine oxidase: from urate catabolism to reperfusion injury to inflammatory signal transduction. *Microcirculation* 9: 161–175, 2002.
34. Moncada S, Palmer RM, and Higgs EA. Nitric oxide: physiology, pathophysiology, and pharmacology. *Pharmacol Rev* 43: 109–142, 1991.
35. Mueller KM, Kornfeld JW, Friedbichler K, Blaas L, Egger G, Esterbauer H, Hasselblatt P, Schlederer M, Haindl S, Wagner KU, Engblom D, Haemmerle G, Kratky D, Sexl V, Kenner L, Kozlov AV, Terracciano L, Zechner R, Schuetz G, Casanova E, Pospisilik JA, Heim MH, and Moriggl R. Impairment of hepatic growth hormone and glucocorticoid

receptor signaling causes steatosis and hepatocellular carcinoma in mice. *Hepatology* 54: 1398–1409, 2011.
36. Nishida J, McCuskey RS, McDonnell D, and Fox ES. Protective role of NO in hepatic microcirculatory dysfunction during endotoxemia. *Am J Physiol* 267: G1135–G1141, 1994.
37. Nurnberger S, Miller I, Duvigneau JC, Kavanagh ET, Gupta S, Hartl RT, Hori O, Gesslbauer B, Samali A, Kungl A, Redl H, and Kozlov AV. Impairment of endoplasmic reticulum in liver as an early consequence of the systemic inflammatory response in rats. *Am J Physiol Gastrointest Liver Physiol* 303: G1373–G1383, 2012.
38. Pacher P, Beckman JS, and Liaudet L. Nitric oxide and peroxynitrite in health and disease. *Physiol Rev* 87: 315–424, 2007.
39. Paletta-Silva R, Rocco-Machado N, and Meyer-Fernandes JR. NADPH oxidase biology and the regulation of tyrosine kinase receptor signaling and cancer drug cytotoxicity. *Int J Mol Sci* 14: 3683–3704, 2013.
40. Parratt JR. Nitric oxide in sepsis and endotoxaemia. *J Antimicrob Chemother* 41 Suppl A: 31–39, 1998.
41. Pelletier MM, Kleinbongard P, Ringwood L, Hito R, Hunter CJ, Schechter AN, Gladwin MT, and Dejam A. The measurement of blood and plasma nitrite by chemiluminescence: pitfalls and solutions. *Free Radic Biol Med* 41: 541–548, 2006.
42. Piskernik C, Haindl S, Behling T, Gerald Z, Kehrer I, Redl H, and Kozlov AV. Antimycin A and lipopolysaccharide cause the leakage of superoxide radicals from rat liver mitochondria. *Biochim Biophys Acta* 1782: 280–285, 2008.
43. Plotnikov EY, Morosanova MA, Pevzner IB, Zorova LD, Manskikh VN, Pulkova NV, Galkina SI, Skulachev VP, and Zorov DB. Protective effect of mitochondria-targeted antioxidants in an acute bacterial infection. *Proc Natl Acad Sci U S A* 110: E3100–E3108, 2013.
44. Postl A, Zifko C, Hartl RT, Ebel T, Miller I, Moldzio R, Redl H, Kozlov AV, Bahrami S, and Duvigneau JC. Transient increase of free iron in rat livers following hemorrhagic-traumatic shock and reperfusion is independent of heme oxygenase 1 upregulation. *Shock* 36: 501–509, 2011.
45. Rocha M, Herance R, Rovira S, Hernandez-Mijares A, and Victor VM. Mitochondrial dysfunction and antioxidant therapy in sepsis. *Infect Disord Drug Targets* 12: 161–178, 2012.
46. Rubbo H, Radi R, Trujillo M, Telleri R, Kalyanaraman B, Barnes S, Kirk M, and Freeman BA. Nitric oxide regulation of superoxide and peroxynitrite-dependent lipid peroxidation. Formation of novel nitrogen-containing oxidized lipid derivatives. *J Biol Chem* 269: 26066–26075, 1994.
47. Schmidt KN, Amstad P, Cerutti P, and Baeuerle PA. The roles of hydrogen peroxide and superoxide as messengers in the activation of transcription factor NF-kappa B. *Chem Biol* 2: 13–22, 1995.
48. Schmittgen TD and Livak KJ. Analyzing real-time PCR data by the comparative C(T) method. *Nat Protoc* 3: 1101–1108, 2008.
49. Schreck R, Albermann K, and Baeuerle PA. Nuclear factor kappa B: an oxidative stress-responsive transcription factor of eukaryotic cells (a review). *Free Radic Res Commun* 17: 221–237, 1992.
50. Schulz E, Wenzel P, Munzel T, and Daiber A. Mitochondrial redox signaling: interaction of mitochondrial reactive oxygen species with other sources of oxidative stress. *Antioxid Redox Signal* 20: 308–324, 2014.
51. Singer M and Brealey D. Mitochondrial dysfunction in sepsis. *Biochem Soc Symp* 66: 149–166, 1999.
52. Skulachev VP. Solution of the problem of energy coupling in terms of chemiosmotic theory. *J Bioenerg* 3: 25–38, 1972.
53. Stanley A, Thompson K, Hynes A, Brakebusch C, and Quondamatteo F. NADPH oxidase complex-derived reactive oxygen species, the actin cytoskeleton, and rho GTPases in cell migration. *Antioxid Redox Signal* 20: 2026–2042, 2014.
54. Szabo C, Ischiropoulos H, and Radi R. Peroxynitrite: biochemistry, pathophysiology and development of therapeutics. *Nat Rev Drug Discov* 6: 662–680, 2007.
55. Taylor DE, Kantrow SP, and Piantadosi CA. Mitochondrial respiration after sepsis and prolonged hypoxia. *Am J Physiol* 275: L139–L144, 1998.
56. Watanabe E, Muenzer JT, Hawkins WG, Davis CG, Dixon DJ, McDunn JE, Brackett DJ, Lerner MR, Swanson PE, and Hotchkiss RS. Sepsis induces extensive autophagic vacuolization in hepatocytes: a clinical and laboratory-based study. *Lab Invest* 89: 549–561, 2009.
57. Weidinger A, Dungel P, Perlinger M, Singer K, Ghebes C, Duvigneau JC, Mullebner A, Schafer U, Redl H, and Kozlov AV. Experimental data suggesting that inflammation mediated rat liver mitochondrial dysfunction results from secondary hypoxia rather than from direct effects of inflammatory mediators. *Front Physiol* 4: 138, 2013.
58. West AP, Brodsky IE, Rahner C, Woo DK, Erdjument-Bromage H, Tempst P, Walsh MC, Choi Y, Shadel GS, and Ghosh S. TLR signalling augments macrophage bactericidal activity through mitochondrial ROS. *Nature* 472: 476–480, 2011.
59. Yu JH, Zhu BM, Riedlinger G, Kang K, and Hennighausen L. The liver-specific tumor suppressor STAT5 controls expression of the reactive oxygen species-generating enzyme NOX4 and the proapoptotic proteins PUMA and BIM in mice. *Hepatology* 56: 2375–2386, 2012.
60. Zhou R, Yazdi AS, Menu P, and Tschopp J. A role for mitochondria in NLRP3 inflammasome activation. *Nature* 469: 221–225, 2011.

Address correspondence to:
Dr. Andrey V. Kozlov
Ludwig Boltzmann Institute for Experimental and Clinical Traumatology
Donaueschingenstrasse 13
Vienna 1200
Austria

E-mail: andrey.kozlov@trauma.lbg.ac.at

Date of first submission to ARS Central, May 16, 2014; date of final revised submission, October 24, 2014; date of acceptance, November 3, 2014.

Abbreviations Used

ADP = adenosine diphosphate
ALT = alanine aminotransferase
AST = aspartate aminotransferase
AU = arbitrary units
BAX = BCL2-associated X protein

Abbreviations Used (Cont.)

BRL3A = buffalo rat liver cell line-3A
BSA = bovine serum albumin
CHOP = C/EBP homology protein
CM = conditioned medium
CO = control
Cybb = cytochrome b(-245)beta subunit od NADPH oxidase (cybb)
cytROS = cytoplasmic reactive oxygen species
DCF-DA = 2′,7′-dichlorofluorescin diacetate
DAF-FM = 4-amino-5-methylamino-2′,7′-difluorofluorescein
EPR = electron paramagnetic resonance
ETC = electron transport chain
H_2O_2 = hydrogen peroxide
HIF1α = hypoxia-inducible factor 1-alpha
i.p. = intraperitoneally
i.v. = intravenously
IL = interleukin
IM = inflammatory mediator
iNOS = inducible nitric oxide synthase
IS = internal standard
LDH = lactate dehydrogenase
L-NMMA = L-NG-monomethyl arginine citrate
LPS = lipopolysaccharide
LSM = laser scanning microscopy
mtAOX = mitochondrial targeted antioxidants
mtROS = mitochondrial reactive oxygen species
mtSOD = mitochondrial superoxide dismutase
ND = not detectable
NF-κB = nuclear factor-κB
NO = nitric oxide
NO-Fe = dinitrosyl iron complexes
NO-Hb = mononitrosyl-hemoglobin-complexes
NOX = NADPH oxidase
NO_x = total NO
$O2^{\bullet-}$ = superoxide radical
$ONOO^-$ = peroxynitrite
PAGE = polyacrylamide gel electrophoresis
qPCR = quantitative polymerase chain reaction
ROS = reactive oxygen species
SDG = succinate dehydrogenase
SEM = standard error of the mean
SIR = systemic inflammatory response
STAT = signal transducers and activators of transcription
TNF = tumor necrosis factor
WBC = white blood cells
XOR = xanthine oxidoreductase